http://www.jstage.jst.go.jp/browse/biophysics

BIOPHYSICS

Vol. 7, pp. 35–49 (2011)
doi: 10.2142/biophysics.7.35

Roles of the C-terminal residues of calmodulin in structure and function

Chihiro Kitagawa[1], Akiko Nakatomi[1], Dasol Hwang[2], Issey Osaka[2], Hiroki Fujimori[3], Hideya Kawasaki[3], Ryuichi Arakawa[3], Yota Murakami[1] and Shinya Ohki[2]

[1]*Department of Chemistry, Faculty of Science, Hokkaido University, N10 W8, Sapporo 060-0810, Japan*
[2]*Center for Nano Materials and Technology (CNMT), Japan Advanced Institute of Science and Technology (JAIST), 1-1 Asahidai, Nomi, Ishikawa 923-1292, Japan*
[3]*Faculty of Chemistry, Materials and Bioengineering, Kansai University, 3-3-35 Yamatecho, Suita, Osaka 564-8680, Japan*

Received March 14, 2011; accepted May 8, 2011

Electrospray ionization mass spectrometry (ESI-MS), circular dichroism (CD), nuclear magnetic resonance (NMR) spectroscopy, flow dialysis, and bioactivity measurements were employed to investigate the roles of the C-terminal residues of calmodulin (CaM). In the present study, we prepared a series of truncated mutants of chicken CaM that lack four (CCMΔ4) to eight (CCMΔ8) residues at the C-terminal end. It was found that CCMΔ4, lacking the last four residues (M145 to K148), binds four Ca^{2+} ions. Further deletion gradually decreased the ability to bind the fourth Ca^{2+} ion, and CCMΔ8 completely lost the ability. Interestingly, both lobes of Ca^{2+}-sturated CCMΔ5 showed instability in the conformation, although limited part in the C-lobe of Ca^{2+}-saturated CCMΔ4 was instable. Moreover, unlike CCMΔ4, structure of the C-lobe in CCMΔ5 bound to the target displayed dissimilarity to that of CaM, suggesting that deletion of M144 changes the binding manner. Deletion of the last five residues (M144 to K148) and further truncation of the C-terminal region decreased apparent capacity for target activation. Little contribution of the last four residues including M145 was observed for structural stability, Ca^{2+}-binding, and target activation. Although both M144 and M145 have been recognized as key residues for the function, the present data suggest that M144 is a more important residue to attain Ca^{2+} induced conformational change and to form a proper Ca^{2+}-saturated conformation.

Key words: truncation, activity, CD, ESI-MS, NMR

Abbreviations: BSA, bovine serum albumin; BBO, broadband observe; CaM, calmodulin; CCM0, intact chicken calmodulin; CCMΔX, a deletion mutant of CCM0 that lacks X C-terminal residues; CD, circular dichroism; CN, calcineurin; EDTA, ethylenediaminetetraacetic acid; EGTA, (ethylenedioxy)diethylenedinitrilotetraacetic acid; ESI, electrospray ionization; FID, free induction decay; HSQC, heteronuclear single quantum correlation spectroscopy; IPTG, isopropyl β-D-1-thiogalactopyranoside; LC, liquid chromatography; MOPS, 3-(*N*-morpholino) propanesulfonic acid; MS, mass spectrometry; NMR, nuclear magnetic resonance; OD, optical density; pNPP, *p*-nitrophenylphosphate; pNPPase, *p*-nitrophenylphosphatase; skMLCK, skeletal muscle myosin light-chain kinase; skMLCKp; a peptide corresponding to the CaM-binding site of skMLCK; smMLCK, smooth muscle myosin light-chain kinase; yCaM, *Saccharomyces cerevisiae* CaM.

Corresponding author: Shinya Ohki, Center for Nano Materials and Technology (CNMT), Japan Advanced Institute of Science and Technology (JAIST), 1-1 Asahidai, Nomi, Ishikawa 923-1292, Japan.
e-mail: shinya-o@jaist.ac.jp

Calmodulin (CaM) is a widely distributed small acidic Ca^{2+}-binding protein composed of 148 amino acid residues, and is a ubiquitous signal transducer connecting cell stimuli to specific biological functions. When the intracellular Ca^{2+} concentration increases, one CaM molecule binds four Ca^{2+} ions. Ca^{2+}-saturated CaM can then bind to and activate various enzymes. More than 100 different CaM target enzymes have been identified. Therefore, CaM is recognized as a regulator of a variety of cellular functions, such as neurotransmitter release and smooth muscle contraction[1–3].

The three-dimensional structure of CaM is well characterized. X-ray crystallographic study has shown that CaM

Figure 1 Amino acid sequences of chicken CaM and its variants. The amino acids are represented by a one-letter code. Only EF4 is aligned in this figure. The red letters indicate the residues in the F-helix, and the blue regions represent Ca^{2+}-binding loops.

has a dumbbell-like structure in which the two globular domains are connected by a long α-helix[4]. Nuclear magnetic resonance (NMR) studies suggest that the middle part of the α-helical linker is somewhat disordered and flexible[5]. Each domain of CaM contains two Ca^{2+}-binding sites with a helix-loop-helix structure, the so-called EF hand motifs. These four Ca^{2+} binding sites are numbered EF1–4, starting from the N-terminus. The C-lobe EF3 and EF4 sites exhibit higher affinity for Ca^{2+}, whereas N-lobe EF1 and EF2 exhibit lower Ca^{2+}-affinity[6]. Binding of Ca^{2+} to CaM induces a conformational change that exposes the hydrophobic residues responsible for target binding to the molecular surface[7–10].

The CaM binding regions of many target enzymes have been identified and characterized. Normally, the CaM binding sites are composed of a continuous stretch of approximately 20–30 amino acid residues[3]. The CaM-binding domain peptides usually form amphiphilic α-helices, and their binding to Ca^{2+}-saturated CaM occurs in a one-to-one stoichiometric ratio[11]. The typical classical structure of a complex between Ca^{2+}-saturated CaM and the target peptide is the wrap-around model[7,8]: the two lobes of Ca^{2+}-saturated CaM become close by bending the flexible part at the middle of the linker and wrap around the target peptide forming an α-helical structure. In this complex, both lobes of Ca^{2+}-saturated CaM bind to the target via the hydrophobic residues exposed on the molecular surface.

CaM is widely distributed in eukaryotes and its amino acid sequences are highly conserved; the only exception identified to date is *Saccharomyces cerevisiae* CaM (yCaM). The sequence homology between yCaM and the CaMs of other species is approximately 60%. The differences are concentrated in the EF4 site of yCaM: two residues are missing and 15 residues are substituted compared to EF4 of chicken CaM[12–14]. Because of such dissimilarity, the EF4 of yCaM does not bind Ca^{2+}. However, it has been reported that the EF4 F-helix of yCaM is essential for target activation[13–16]. Thus, it remains unclear how the C-terminal residues of CaM contribute to its structure and function. In this study, we investigated the roles of the C-terminal residues of CaM by using a series of deletion mutants of intact chicken CaM (CCM0); for example, CCMΔ4 is lacking the four C-terminal residues of CCM0 (Fig. 1). We measured their capacity to bind Ca^{2+} by mass spectrometry (MS) and flow-dialysis. Circular dichroism (CD) was employed to monitor the Ca^{2+}-induced conformational change. In addition, we obtained various NMR data to discuss their structural characteristics in the absence and presence of Ca^{2+} and/or target. Their biological activities for calcineurin (CN) were also examined.

Materials and Methods

Samples

The DNA fragments encoding CaM and its variants were inserted into the pET30b(+) plasmid. Recombinant chicken CaM and its deletion mutants were expressed in *Escherichia coli* BL21.

Unlabeled CaM and its variants were expressed and purified as reported previously[17]. Uniform ^{15}N-labeled CaM and its variants were expressed in *E. coli* grown in M9 medium containing $^{15}NH_4Cl$ as the sole source of nitrogen. To enhance cell growth and protein production, 1 g/L ISOGRO (ISOTEC Co.) was added to the culture medium. Selectively labeled-[^{13}C]-*methyl*-Met CaM and its variants were obtained as follows. For protein expression, *E. coli* was cultured in unlabeled M9 medium until the optical density (OD) at 600 nm (A_{600}) reached 0.3. Subsequently, an amino acid mixture of Tyr, Phe, Leu, Ile, Val, and [^{13}C]-*methyl*-Met (100 mg each per liter of culture medium) was added to the medium. Protein production was induced by adding isopropyl β-D-1-thiogalactopyranoside (IPTG) to the medium at A_{600} of 0.7. The bacteria were harvested after shaking for 4 h at 37°C. Purification of proteins for NMR was performed by using previously reported methods[17,18].

Calcineurin (CN) was extracted from scallop testes by using buffer A (20 mM imidazole-HCl [pH 7.0], 1 mM (ethylenedioxy)diethylenedinitrilotetraacetic acid [EGTA], 2 mM $MgCl_2$, 50 mM NaCl, 14 mM 2-mercaptoethanol, 0.1 mM diisopropylfluorophosphate, 0.1 mM phenylmethylsulfonyl fluoride, 1 mM benzamidine) and fractionated using ammonium sulfate at 35–55% saturation. The precipitate was homogenized, adjusted to 30% saturation with ammo-

nium sulfate in buffer B (20 mM imidazole-HCl [pH 7.0], 1 mM EGTA, 2 mM $MgCl_2$, 14 mM 2-mercaptoethanol), and applied to a TOYOPEARL Phenyl-650M column (Tosoh). The column was washed with buffer B containing ammonium sulfate at 30% saturation, and eluted with buffer B containing ammonium sulfate at 15% saturation. The concentration of $CaCl_2$ in the eluate was adjusted to 5 mM, and this eluate was applied to a CaM-Sepharose CL-4B column equilibrated with buffer C_1 (buffer C [20 mM Tris-HCl, 2 mM $MgCl_2$, 14 mM 2-mercaptoethanol, pH 8.0] containing 80 mM NaCl and 5 mM $CaCl_2$), and then buffer C_2 (buffer C containing 500 mM NaCl and 0.2 mM $CaCl_2$). The column was first washed with buffer C_2 and then with buffer C_3 (buffer C containing 80 mM NaCl and 0.2 mM $CaCl_2$). It was finally eluted using buffer C_4 (buffer C containing 80 mM NaCl and 1 mM EGTA). The eluate was applied to a Cellufine A-500-m (Chisso) column equilibrated with buffer C_4. The column was washed with buffer C_4 and developed using a linear gradient of 80–300 mM NaCl. The fractions that had CN phosphatase activity were collected and dialyzed against buffer D (buffer C containing 80 mM NaCl, 1 mM EGTA, and 50% glycerol), and stored at −20°C.

For the NMR studies, we employed a chemically synthesized 26-residue peptide, purchased from a company (invitrogen), encompassing the CaM-binding region of skeletal muscle myosin light-chain kinase (skMLCK), *i.e.*, skMLCKp (KRRWKKNFIAVSAANRFKKISSSGAL)[3].

Liquid chromatography-mass spectrometry (LC-MS)

LC-MS experiments were employed to clarify the number of Ca^{2+} ions bound to CaM and its variants. LC-MS analyses were performed in a negative-ion mode by using an electrospray ionization (ESI)-orbitrap mass spectrometer (Exactive, Thermo Fisher Scientific) combined with HPLC (ACCELA, Thermo Fisher Scientific). The LC experiments were carried out with an Inertsil ODS-SP column (2.1 × 150 mm, 3 μm; GL Science). Concentration of all samples was adjusted as 30 μM. Binary mobile phases A (10 mM ammonium acetate and 10 μM calcium acetate aqueous at pH 6.6) and B (97% methanol aqueous with 10 mM ammonium acetate and 10 μM calcium acetate at pH 7.6) were used at a flow rate of 0.2 mL/min, and the gradient was controlled as follows: from 0% B (0–1 min) to 100% B (1–11 min), held at 100% B (11–17 min).

Ca^{2+}-binding assay

Ca^{2+} binding to the samples was measured by flow dialysis using a previously reported method[19,20] with a buffer containing 0.1 M NaCl and 20 mM 3-(*N*-morpholino)propanesulfonic acid (MOPS)-NaOH (pH 7.0). For each sample, we tried the measurements at high and low (120 and 20 μM) concentrations. The experiments were performed at 25°C. Results were analyzed by fitting to Adair's equation using GraphPad Prism (GraphPad Software, San Diego). The results were fitted to a four-site model [1], except for the result for CCMΔ8, which was fitted to a three-site model [2].

$$y = (x/K_1 + 2x^2/K_1K_2 + 3x^3/K_1K_2K_3 + 4x^4/K_1K_2K_3K_4) / (1 + x/K_1 + x^2/K_1K_2 + x^3/K_1K_2K_3 + x^4/K_1K_2K_3K_4). \quad [1]$$

$$y = (x/K_1 + 2x^2/K_1K_2 + 3x^3/K_1K_2K_3) / (1 + x/K_1 + x^2/K_1K_2 + x^3/K_1K_2K_3). \quad [2]$$

Where y is the moles of bound Ca^{2+}, x is the concentration of free Ca^{2+}, and K_1–K_4 are the macroscopic dissociation constants.

CD experiments

CD spectra were recorded at 250–200 nm by using a JASCO 500A spectropolarimeter with a 1-mm optical path length quartz cell. The CD measurements were performed at 25°C with 0.2 mg/mL purified protein dissolved in a buffer containing 20 mM Tris-HCl (pH 8.0), and 1 mM $CaCl_2$ or EGTA.

NMR experiments

Protein samples for NMR were dissolved in 20 mM phosphate buffer containing 100 mM KCl and 10 mM $CaCl_2$ or ethylenediaminetetraacetic acid (EDTA). The sample concentration was about 0.6 mM except for ^{113}Cd-NMR experiments. For ^{113}Cd-NMR experiments, sample concentration was approximately 1.2 mM. The solvent contained 10% D_2O for the NMR lock. The pH of the samples used for ^{113}Cd-NMR and for other experiments was adjusted to 6.5 and 7.0, respectively, using a direct-reading pH meter. The sample temperature was maintained at 25°C during the NMR experiments. The ^{1}H-^{15}N HSQC data were recorded on a Varian INOVA 750 spectrometer with a z-axis gradient triple-resonance probe. The one-dimensional ^{1}H and two-dimensional ^{1}H-^{13}C correlation experiments were performed on a Bruker AVANCE III 800 spectrometer with a TCI cryogenic probe. The ^{113}Cd-NMR data were obtained using a Bruker AVANCE III 500 spectrometer with a broadband-observe (BBO) probe. All free induction decay (FID) data were processed and displayed using NMRPipe[21].

Biological activity

The activity of the CaM-target, CN, was measured in the presence of CaM and its variants. The buffer components were as follows: 100 mM Tris-HCl (pH 8.5), 100 mM NaCl, 10 mM $MgCl_2$, 0.4 mM $CaCl_2$, 7 mM 2-mercaptoethanol, 0.2 mg/mL bovine serum albumin (BSA), 5 mM *p*-nitrophenylphosphate (pNPP), and 5 nM scallop CN. All the experiments were performed at 25°C.

Results

Number of Ca^{2+} ions bound to CaM and the variants

We conducted LC-ESI-MS experiments to clarify the number of Ca^{2+} ions bound to CaM and its variants. The results

are shown in Figure 2. The protein sample was passed through a reverse phase column with a mobile phase solvent containing 10 μM Ca^{2+}. Thus, the results obtained here suggest the number of Ca^{2+} ions bound to CaM and its variants in the presence of 10 μM free Ca^{2+}. The peaks appearing at different retention times were subsequently subjected to ESI-MS analyses. For all samples, the LC peaks in the ESI-MS spectra at a retention time of approximately 10.6 min show $[protein+4Ca\text{-}nH]^{(n-8)-}$ ion. Another peak for CCMΔ5–7 appearing at a later retention time shows $[variant+2Ca\text{-}nH]^{(n-4)-}$ and $[variant+3Ca\text{-}nH]^{(n-6)-}$. When the two peaks were observed in the LC-MS chromatogram, it was found that the former peak was related to the CaM (or variant) with a larger number of Ca^{2+} ions. Ca^{2+}-binding to CaM (or variants) is tight and the on-off exchange rate is thought to be slow enough to separate the $4Ca^{2+}$-bound form from the

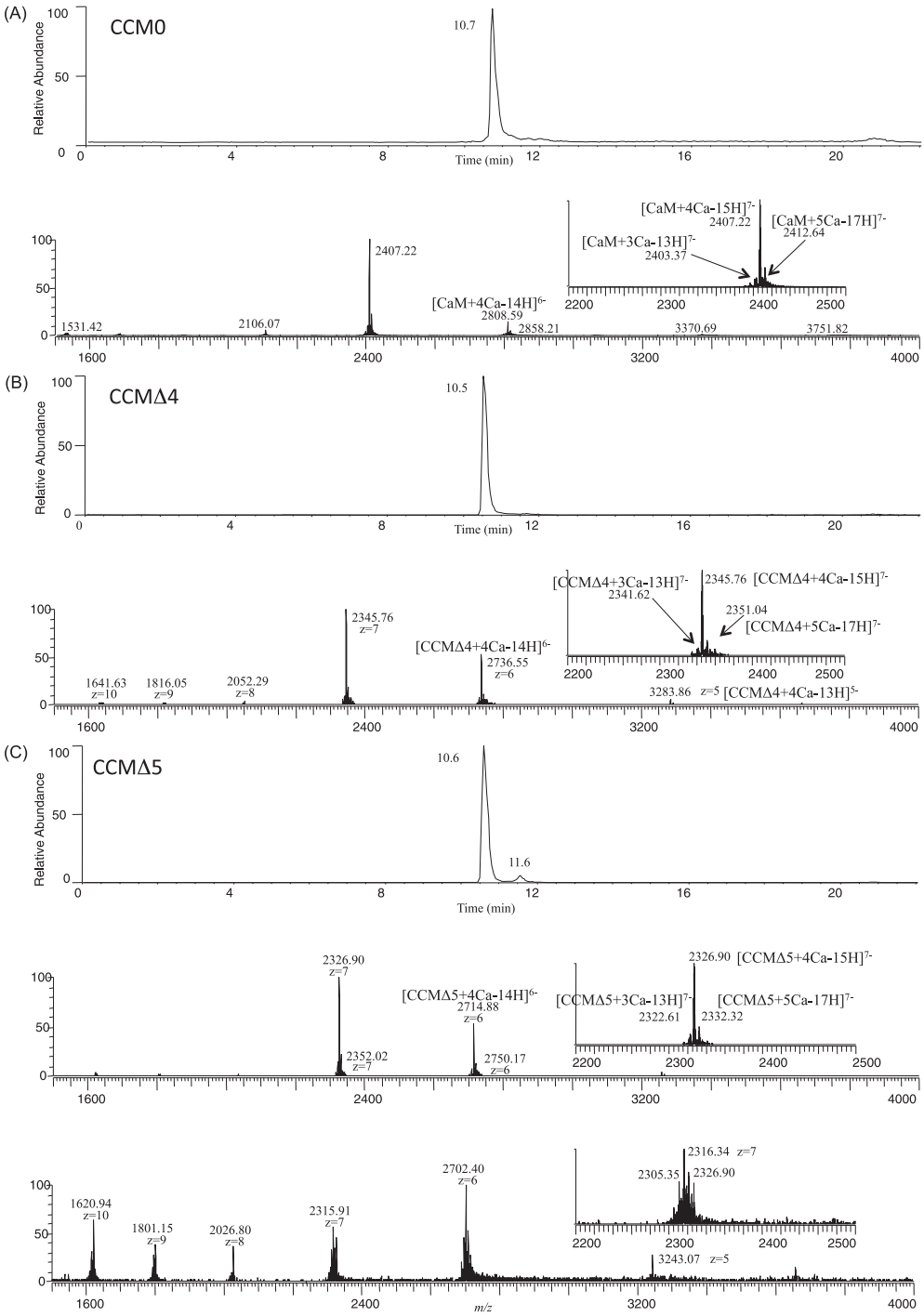

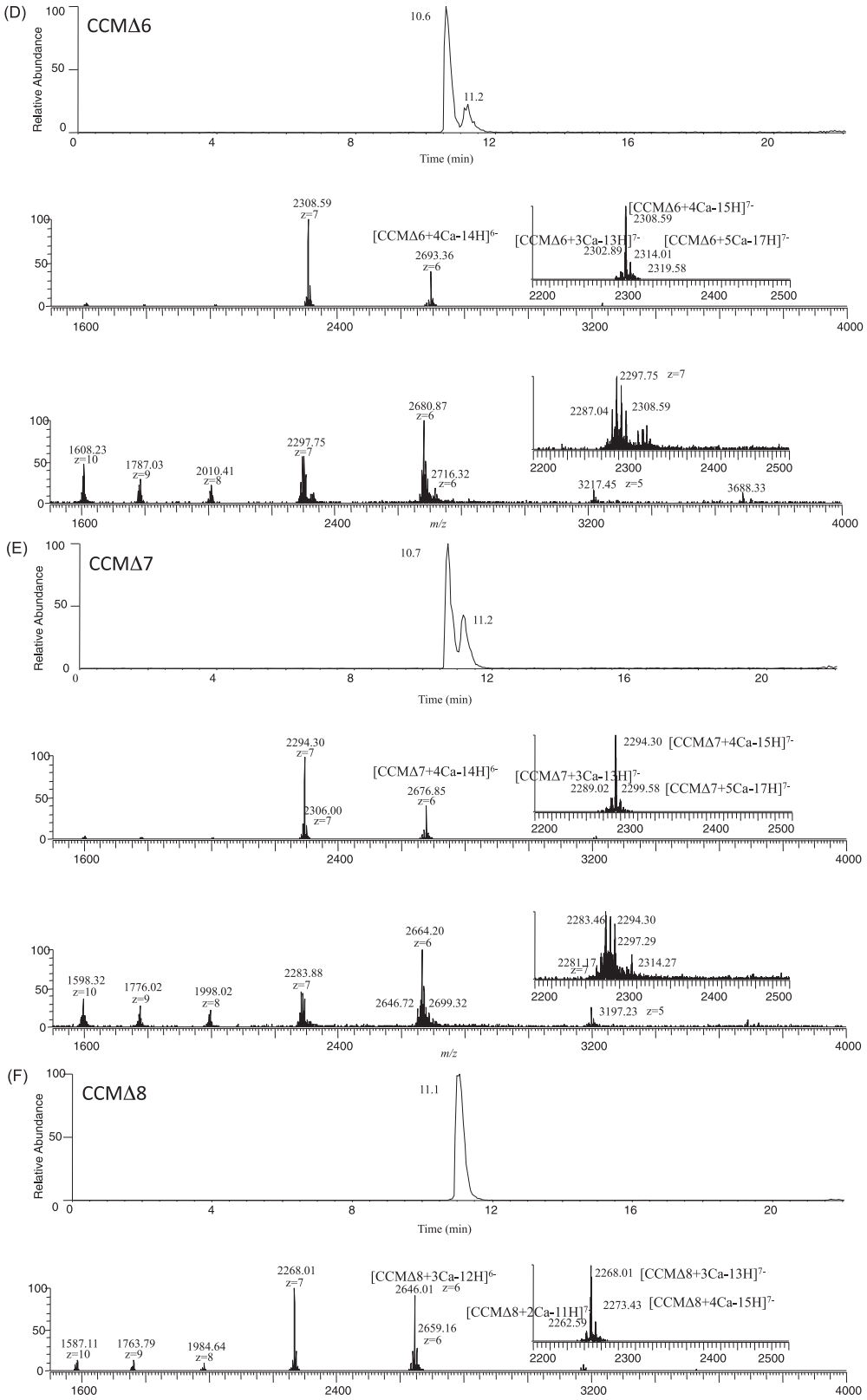

Figure 2 Identification of the number of bound Ca^{2+} ions. LC-ESI-MS data for CCM0 (A), CCMΔ4 (B), CCMΔ5 (C), CCMΔ6 (D), CCMΔ7 (E), and CCMΔ8 (F) are shown. Elution pattern of LC (top), MS of first fraction (middle), and MS of second fraction (bottom) are depicted for each sample. CCM0 (panel A) and CCMΔ4 (panel B) have only one elution peak related to $4Ca^{2+}$-bound form, and CCMΔ8 (panel F) also has only one elution peak of $3Ca^{2+}$-bound form. The molecular mass (Da) of each protein is calculated as follow: 16706.76 (CCM0), 16274.84 (CCMΔ4), 16143.65 (CCMΔ5), 16015.52 (CCMΔ6), 15916.39 (CCMΔ7), and 15769.21 (CCMΔ8).

species with smaller number of Ca^{2+} ions.

As shown in Figure 2, the results clearly indicate that CCM0 and CCMΔ4 bind four Ca^{2+} ions. In contrast, the LC elution pattern for CCMΔ5 has two peaks. The large fraction that eluted at 10.6 min in the LC experiment contained the $4Ca^{2+}$-bound form. The succeeding small peak in the LC experiment was related to $3Ca^{2+}$- and $2Ca^{2+}$-bound forms. Thus, almost all CCMΔ5 molecules were in $4Ca^{2+}$-bound form but very few were in $3Ca^{2+}$- and $2Ca^{2+}$-bound forms. Similar data for CCMΔ5, CCMΔ6, and CCMΔ7 show that they can still bind four Ca^{2+} ions, although some of them become $3Ca^{2+}$- and $2Ca^{2+}$-bound states. The intensity of the LC elution peaks suggests that 82 and 76% of the molecules were in $4Ca^{2+}$-bound states for CCMΔ6 and CCMΔ7, respectively. Finally, the LC experiment for CCMΔ8 did not have an elution peak at ~10.6 min related to the $4Ca^{2+}$-bound form, and only had a peak at 11.1 min. The MS result of the elution peak at 11.1 min indicates that CCMΔ8, the shortest mutant in this study, does not bind the fourth Ca^{2+} ion. Because CCMΔ8 only has three residues for the EF4 F-helix, it seems too short to form a stable helix. This is probably the reason why CCMΔ8 binds only three Ca^{2+} ions.

Affinity of Ca^{2+}

Next, we measured the Ca^{2+}-affinity of CaM and the variants. The results of the flow dialysis experiments with CaM and a series of variants are shown in Figure 3. The results indicate that all of the variants are less sensitive than CCM0 to Ca^{2+}; all these variants bind at least three Ca^{2+} ions. Although very high Ca^{2+} concentrations may have a tendency to lead to great ambiguity in the flow dialysis data, unclear results could be caused by the truncated EF4. Interestingly, EF3 can bind Ca^{2+} in all variants, although it is coupled with EF4 to form the C-lobe.

These results seem to be inconsistent with those obtained by LC-ESI-MS, but it is possible that the difference was caused by different salt conditions: flow dialysis was performed with a buffer containing 0.1 M NaCl, but LC-ESI-MS was carried out without salt due to experimental limitation. Practically, it had been reported that Ca^{2+}-binding of CaM depends on the ion strength of the sample solution[22].

We tried to estimate the Ca^{2+} dissociation constants of intact CaM and its variants. The estimated values are summarized in Table 1. Because Ca^{2+}-binding occurs in equilibrium, it was thought that four Ca^{2+} were bound to the proteins, except for CCMΔ8. For all variants except for CCMΔ8, three of four EF hand sites apparently showed similar Ca^{2+}-affinity and the remaining one site, probably EF4, had weaker affinity for Ca^{2+}. Although the curve fitting was rough because of a small number of data points for the variants, we can interpret the results qualitatively. The data suggest that the truncation destabilizes EF4 and decreases its Ca^{2+}-affinity, which affects the Ca^{2+}-affinity of EF3 in the C-lobe, and as a result, three of the four EF hand sites (EF1-3) develop similar Ca^{2+}-affinity.

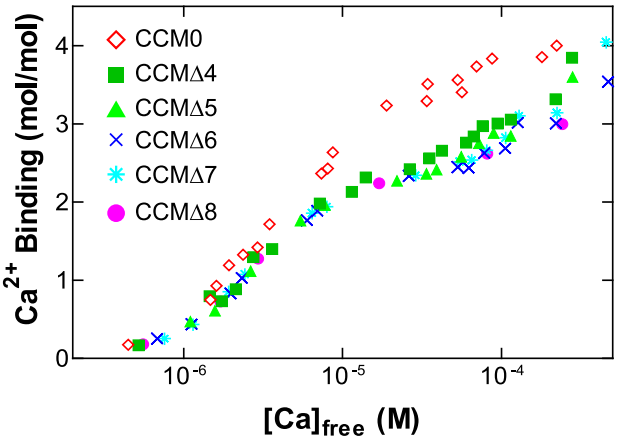

Figure 3 Ca^{2+}-binding by CaM and its variants. The flow dialysis results for CCM0, CCMΔ4, CCMΔ5, CCMΔ6, CCMΔ7, and CCMΔ8 are shown. The experimental conditions have been described in detail in Materials and Methods.

CD experiments

The global conformation and Ca^{2+}-induced conformational changes in CaM and its variants were monitored using CD. The CD spectra of CaM and its deletion mutants in the absence and presence of Ca^{2+} are shown in Figure 4. The spectra of apo and Ca^{2+}-bound CCM0 were greatly different. Ca^{2+}-induced conformational change caused this spectral difference for CCM0. Although CCMΔ4 displayed a large spectral change similar to that observed for CCM0, a not so large spectral change was detected for CCMΔ5. Therefore, we can point out that deletion of M144 causes this drastic difference. Like CCMΔ5, the shorter mutants lacking 6, 7, and 8 residues at the C-terminus did not exhibit

Table 1 Estimated macroscopic Ca^{2+} dissociation constants of CaM and its variants

sample	K_1 (M)	K_2 (M)	K_3 (M)	K_4 (M)
CCM0	$(2.8\pm1.9)\times10^{-6}$	$(1.7\pm2.7)\times10^{-6}$	$(8.0\pm3.3)\times10^{-6}$	$(2.5\pm0.6)\times10^{-5}$
CCMΔ4	$(1.9\pm5.0)\times10^{-5}$	$(2.7\pm7.1)\times10^{-7}$	$(5.9\pm1.9)\times10^{-5}$	$(1.2\pm40)\times10^{-4}$
CCMΔ5	$(4.4\pm14)\times10^{-5}$	$(1.2\pm4.1)\times10^{-7}$	$(9.3\pm2.2)\times10^{-5}$	$(1.4\pm41)\times10^{-4}$
CCMΔ6	$(1.5\pm1.9)\times10^{-5}$	$(3.7\pm4.8)\times10^{-7}$	$(8.7\pm1.9)\times10^{-5}$	$(3.4\pm97)\times10^{-4}$
CCMΔ7	$(6.4\pm56)\times10^{-5}$	$(7.8\pm0.7)\times10^{-8}$	$(1.6\pm90)\times10^{-4}$	$(9.8\pm6.0)\times10^{-5}$
CCMΔ8	$(7.7\pm9.4)\times10^{-6}$	$(7.2\pm8.9)\times10^{-7}$	$(3.7\pm1.1)\times10^{-5}$	

All constants were estimated by curve-fitting to Adair's equation using the data shown in Figure 3. For CCMΔ8, three Ca^{2+} binding sites were assumed.

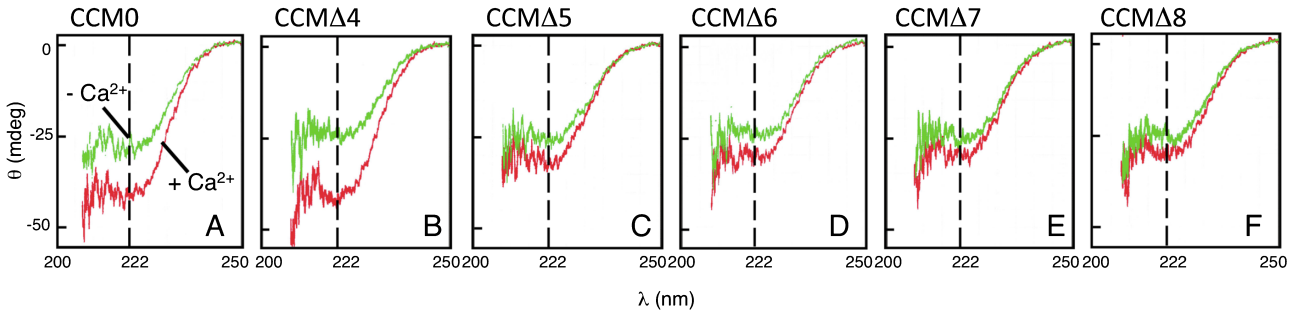

Figure 4 CD spectra of CaM and its variants. The green and red curves indicate the CD data with and without Ca^{2+}, respectively. CCM0 (A), CCMΔ4 (B), CCMΔ5 (C), CCMΔ6 (D), CCMΔ7 (E), and CCMΔ8 (F).

significant spectral change induced by Ca^{2+}-binding. This implies that further truncation of the C-terminal region increases insensitivity to Ca^{2+} and relates to reduced Ca^{2+}-induced structural changes.

Ca^{2+} titration

Extensive structural studies were carried out through NMR experiments. In this study, we employed CCMΔ4 and CCMΔ5 for the NMR analyses because their CD spectral change upon binding of four Ca^{2+} ions is different: the result for CCMΔ4 was similar to that of CCM0, but CCMΔ5 was different. Thus, it was expected that a comparison of the NMR data with CCM0 would give fundamental information about the role of the C-terminal residues, especially for M144.

For the first NMR analysis, we demonstrated one dimensional ^{1}H-NMR experiments to clarify the Ca^{2+}-binding order among the four EF hands in CaM and its variants. Figure 5 indicates stacked plots of the down field amide region in one-dimensional ^{1}H-NMR spectra of CCMΔ4 and CCMΔ5 through the Ca^{2+}-titration.

In the data for CCMΔ4, peaks of G25 and G61 in the apo-form decreased in intensity with increasing Ca^{2+} concentration. These two peaks disappeared around [Ca^{2+}]/[CCMΔ4] = 2. Alongside the disappearance, a new peak appeared at 10.67 ppm, which was the overlapped resonances of G25, G61, and G98 in the Ca^{2+}-bound form. Peaks of G25, G61, and G98 are good probes of EF1, 2, and 3, respectively.

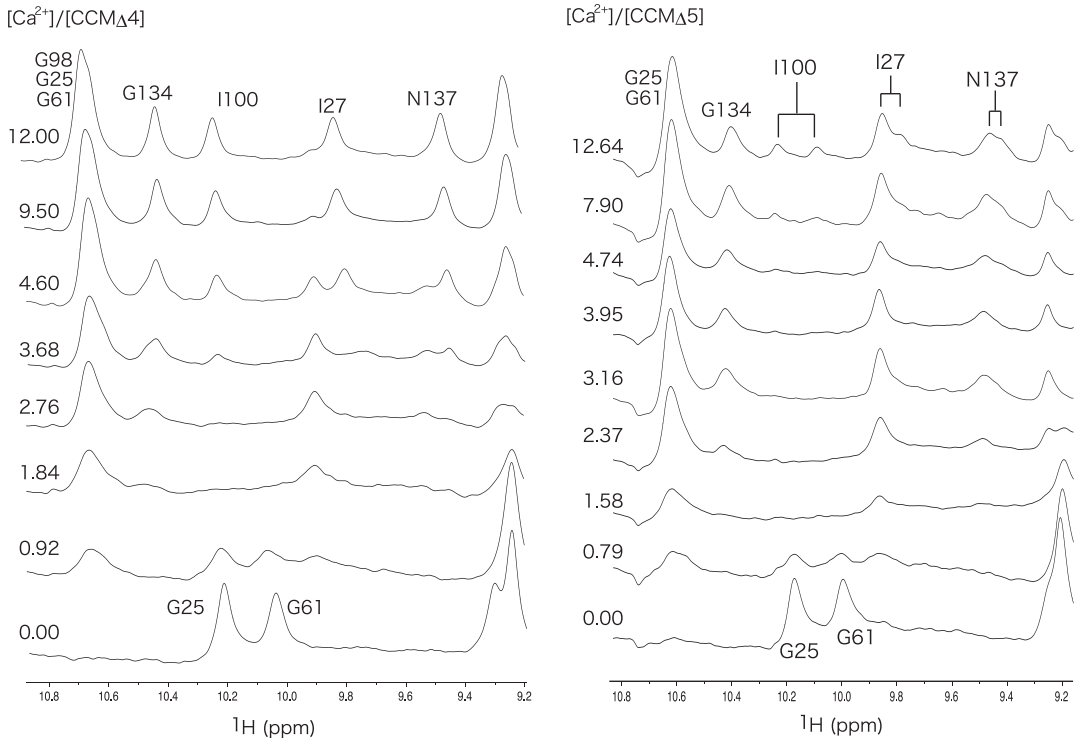

Figure 5 ^{1}H-NMR spectra of CaM and its variants at various concentration of Ca^{2+}. Panels A and B are results of CCMΔ4 and CCMΔ5, respectively. The numbers shown in the two figures indicate the [Ca^{2+}]/[variant] ratio. The assignments were according to Figure 6.

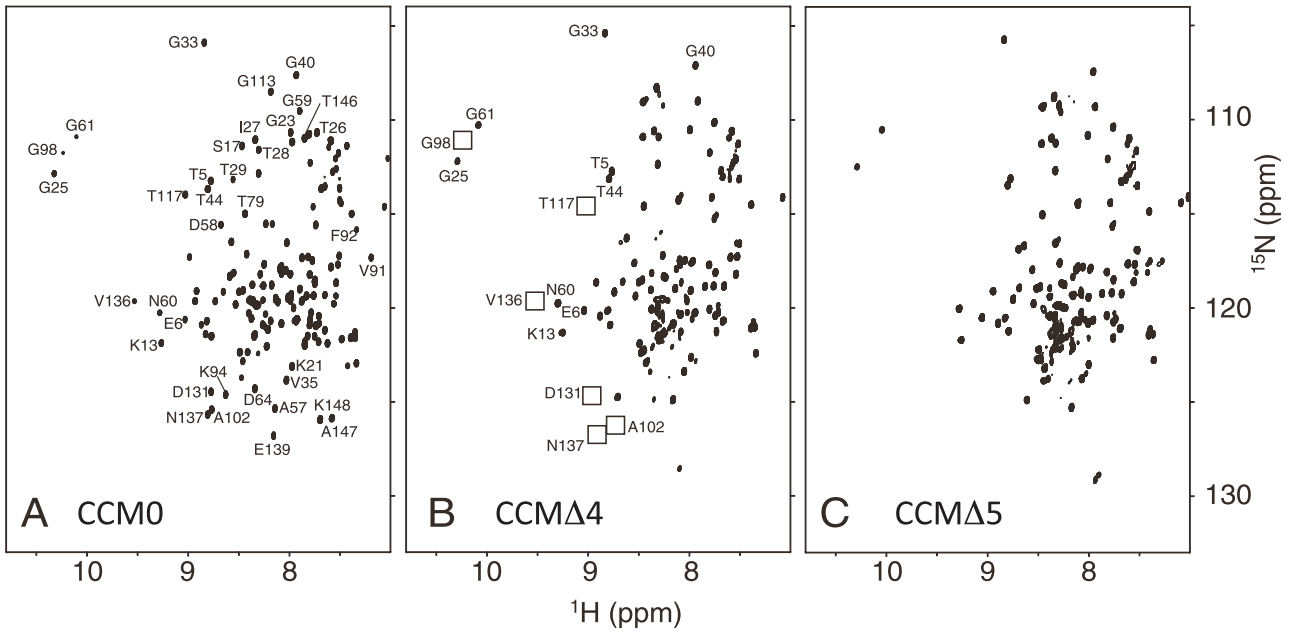

Figure 6 ^{1}H-^{15}N HSQC of uniformly ^{15}N-labeled CaM and its variants in the absence of Ca^{2+}. The NMR spectra for CCM0 (A), CCMΔ4 (B), and CCMΔ5 (C) were recorded at a ^{1}H frequency of 750 MHz. For clarity, only selected residues are labeled with their residue name and number. The positions of the peaks that are absent in panel (B) have been labeled using boxes.

Thus, the NMR spectral change indicates that EF1, 2, and 3 have similar Ca^{2+} affinity. At very high concentration of Ca^{2+}, an additional peak corresponding to G134 involved in EF4 appeared at slightly higher field than that of the overlapped three Gly's peaks. Interestingly, the peak of N137 located in EF4 appeared in the two-step manner with increasing concentration of Ca^{2+}. At lower Ca^{2+} concentration, the peak of N137 in the Ca^{2+}-bound form appeared at 9.54 ppm, but this peak disappeared at very high Ca^{2+} concentration. Finally, a new N137 peak appeared at 9.48 ppm. Similar two-step spectral change was observed for I27 appearing at 9.91 and 9.82 ppm. This spectral change was even observed at much higher Ca^{2+}-concentration. The spectral change strongly suggests that conformational transition in both lobes of CCMΔ4 induced by Ca^{2+}-binding is not achieved in a simple two-state exchange.

The spectral change of CCMΔ5 was more complicated. It was hard to assign which sites showed higher or lower Ca^{2+} affinity. Split peaks were observed for I27, I100, and N137 at higher Ca^{2+} concentration, suggesting that both the N- and C-domain of CCMΔ5 in the presence of Ca^{2+} are not in a single conformation. Such structural heterogeneity makes it difficult to analyze spectral change in detail.

^{1}H-^{15}N HSQC

For the next NMR study, we performed heteronuclear two-dimensional ^{1}H-^{15}N HSQC experiments to obtain detailed information on the global structures. The ^{1}H-^{15}N HSQC spectra of CaM and its variants in the absence of Ca^{2+} are shown in Figure 6. Several peaks observed in the NMR spectrum of apo-CCM0 disappeared within that of apo-CCMΔ4. The missing peaks included G98, A102, T117, D131, V136, and N137, all of which are located in the C-lobe. Although the deletion was performed at EF4, the four-residue truncation induced a global conformational change in the whole C-lobe, that is, both EF3 and EF4 were affected. These results seem to be reasonable because EF3 and EF4 form a globular domain. In contrast, the peaks that resonated from the residues in the N-lobe of apo-CCMΔ4 appeared at chemical shift positions identical to those observed in the spectrum of apo-CCM0. The four-residue deletion at the C-terminus induces structural changes at the C-lobe, but not at the N-lobe. The NMR spectra of apo-CCMΔ4 and apo-CCMΔ5 were very similar, suggesting that their conformation is very similar.

The ^{1}H-^{15}N HSQC spectra of CaM and its variants in the presence of excess Ca^{2+} are shown in Figure 7. The samples were expected to be in Ca^{2+}-saturated forms in this condition. The NMR spectra of all samples were changed by the addition of Ca^{2+}. Therefore, the results clearly suggest that binding of Ca^{2+} to CCMΔ4 and CCMΔ5 induces conformational changes. The spectrum of Ca^{2+}-bound CCMΔ4 was very close to that of Ca^{2+}-bound CCM0. Thus, the four-residue truncation does not disturb the overall structure of CaM. Surprisingly, I130, V136, and N137, which belong to EF4, still resonated at proper chemical shifts. However, the residues, such as F141, which are located in the F-helix of EF4 in Ca^{2+}-bound CCMΔ4, disappeared. The NMR data regarding EF4 in Ca^{2+}-bound CCMΔ4 suggests that only the F-helix is destabilized. Unlike the residues forming EF4, all

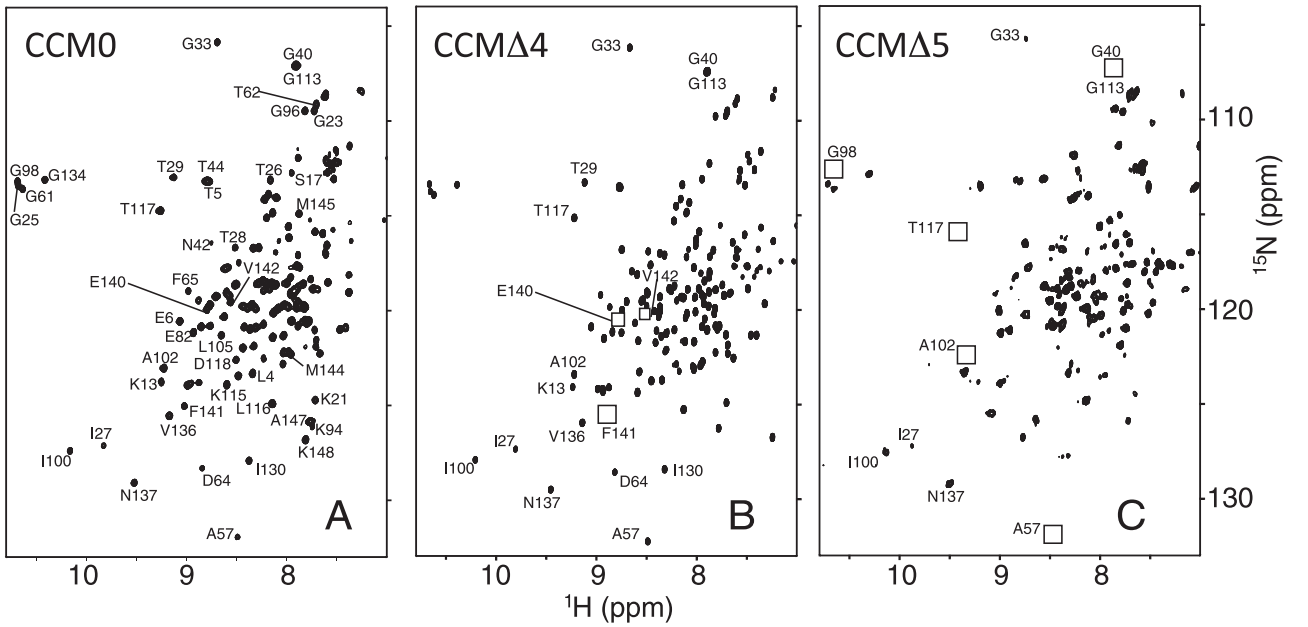

Figure 7 ^{1}H-^{15}N HSQC of uniformly ^{15}N-labeled CaM and its variants in the presence of Ca^{2+}. The NMR spectra for CCM0 (A), CCMΔ4 (B), and CCMΔ5 (C) were recorded at a ^{1}H frequency of 750 MHz. For clarity, only selected residues are labeled with their residue name and number. The positions of the peaks that are absent in panels (B) and (C) have been labeled using boxes.

the residues forming EF3, for example, Ile100, Ala102, and G113 (Figure 7B) were observed at their proper chemical shifts. Unlike apo-form, the entire EF3 site keeps its native conformation in the Ca^{2+}-bound CCMΔ4, indicating that the disorder in EF4 F-helix does not affect the structure of EF3. This finding is completely different to that observed for apo-CCMΔ4, suggesting that Ca^{2+} binding may enhance the structural stability of the C-lobe.

In contrast to CCMΔ4, the NMR spectrum of Ca^{2+}-bound CCMΔ5 was largely different from that of Ca^{2+}-bound CCM0. Some peaks became broad or weak, others were missing, and some new peaks appeared in the central region of the ^{1}H-^{15}N HSQC spectra. Therefore, the structure of Ca^{2+}-bound CCMΔ5 is heterogeneous. It is noteworthy that the residues located in the N-lobe were also affected. For example, peak A57 was missing, and peak G33 became very weak. Therefore, it can be concluded that the 5-residue truncation introduced at the C-terminus disturbed the conformation of both lobes of CCMΔ5 in the presence of Ca^{2+}. This is totally different from the results obtained for CCMΔ4. The fifth residue from the C-terminus (M144) is the key for preserving the overall structure of Ca^{2+}-bound CaM, although it does not play a critical role in the apo form.

The downfield-shifted I27, I100, and N137 peaks of Ca^{2+}-bound CCMΔ5 became weak, broad, and/or duplicated (Figure 8). The results are completely dissimilar to those of CCM0 and CCMΔ4. The spectrum strongly suggests that Ca^{2+}-bound CCMΔ5 is in conformational equilibrium, whereas Ca^{2+}-bound CCMΔ4 has a relatively stable conformation.

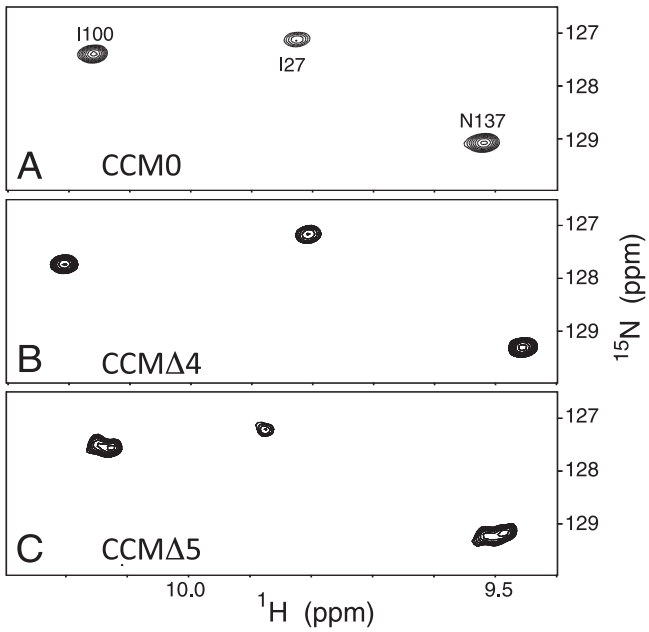

Figure 8 Downfield-shifted regions in ^{1}H-^{15}N HSQC of uniformly ^{15}N-labeled CaM and its variants in the presence of Ca^{2+}. CCM0 (A), CCMΔ4 (B), and CCMΔ5 (C).

^{1}H-^{13}C HSQC of Met residues

To simplify the NMR spectra and to obtain side chain structural information, we focused on the Met side chain signals of CaM. The structural changes caused by binding of Ca^{2+} and/or a target were monitored by ^{1}H-^{13}C HSQC of

selectively labeled-[^{13}C]-*methyl*-Met CaM and its variants.

CaM molecule contains nine Met residues at each of the following positions: 36, 51, 71, 72, 76, 109, 124, 144, and 145. Previous studies have indicated that these Met residues are exposed to solvent upon Ca^{2+} binding and that the unbranched side chains are involved in target binding[7,8]. Hence, we focused on the Met residues. Another motivation to monitor the Met methyl groups is due to the simplicity of NMR measurements. Generally, the methyl group shows high sensitivity and gives a narrow line shape in ^{1}H-^{13}C correlation experiments because of the number of attached protons and their rotation. Thus, methyl groups are adequately sensitive probes for NMR studies. Furthermore, in the case of Met, the carbon atom of the methyl group is attached to a sulfur atom. Thus, spin decoupling to eliminate $^{1}J_{CC}$ coupling by using constant time or band-selective pulses is unnecessary during the ^{13}C evolution period. Hence, the methyl groups of the nine Met residues have been utilized as powerful practical probes in NMR studies on CaM[23].

In this study, a chemically synthesized 26-residue peptide, corresponding to the CaM-binding domain of skeletal muscle myosin light-chain kinase (skMLCKp), was used as the CaM target mainly because of the following reasons. First, it is known that the tight binding of skMLCKp to CaM occurs in a 1:1 stoichiometric ratio that depends on the binding of Ca^{2+} to CaM. Second, previous NMR studies have reported ^{1}H and ^{13}C chemical shifts of all Met signals in CaM in the Ca^{2+}-free, Ca^{2+}-bound, and skMLCKp-complex forms[24].

The ^{1}H-^{13}C HSQC results for CCM0, CCMΔ4, and CCMΔ5 are shown in Figure 9. All the resonance assignments for variants displayed in panels D–I are according to a comparison with the spectra for CCM0. The results for the Ca^{2+}-free forms are shown in panels A, D, and G. It is clear that the peaks that resonated from the residues in Ca^{2+}-free N-lobe were not affected by the truncation of four or five residues at the C-terminus, indicating that this deletion does not affect the structure of the N-lobe in the absence of Ca^{2+}. These results are consistent with those of the ^{1}H-^{15}N HSQC. Unlike the Met residues in the N-lobe, the peaks of M109, M124, and M144 in the C-lobe of CCMΔ4 and CCMΔ5 were shifted by the truncation. Thus, the conformation of the Ca^{2+}-free C-lobe of the variants is different from that of CCM0. These findings are also consistent with the above-mentioned results for ^{1}H-^{15}N HSQC.

The spectra of the Ca^{2+}-bound forms of CCM0, CCMΔ4, and CCMΔ5 are shown in panels B, E, and H of Figure 9, respectively. In contrast to the Ca^{2+}-free forms, Ca^{2+}-bound CCMΔ4 and CCMΔ5 displayed different spectra. In the C-lobe of Ca^{2+}-bound CCMΔ4, the peaks of M109 and M124 in EF3 appeared at almost identical chemical shift positions compared with those of Ca^{2+}-bound CCM0, suggesting that their local magnetic environment is similar. The peak of M144 in Ca^{2+}-bound CCMΔ4 resonated at higher field in the ^{13}C dimension compared with that of CCM0. Thus, in the presence of Ca^{2+}, the conformation of EF4 in the C-lobe of CCMΔ4 is different from that of CCM0, but EF3 maintains its original conformation. This result is also consistent with that of ^{1}H-^{15}N HSQC.

The spectral change detected in Ca^{2+}-bound CCMΔ5 was greater than that detected in Ca^{2+}-bound CCMΔ4. The peaks of six Met residues, except M124, could be assigned on the basis of their chemical shift values. However, eight peaks remained unassigned, although CCMΔ5 has only seven Met residues. This result strongly suggests that the Ca^{2+}-bound CCMΔ5 has multiple conformations. Taken together with the results of the ^{1}H-^{15}N HSQC, we conclude that both lobes of Ca^{2+}-saturated CCMΔ5 exist in multiple conformations. The conformational equilibrium is expected to be slow in the NMR time scale because of their sharp line shape.

The NMR spectra of the complexes are shown in panels C, F, and I of Figure 9. The spectrum of CCMΔ4 was very similar to that of CCM0. This indicates that both lobes of Ca^{2+}-bound CCMΔ4 simultaneously interact with skMLCKp and that the conformation of Ca^{2+}-bound CCMΔ4 is similar to that of Ca^{2+}-bound CCM0. Thus, the four-residue truncation has very limited effects on forming the skMLCKp-bound complex. Similar to CCM0 and CCMΔ4, CCMΔ5 gave a clear NMR spectrum with seven peaks—corresponding to the exact number of Met residues in CCMΔ5. Consequently, complexed CCMΔ5 has a stable single conformation as opposed to the Ca^{2+}-bound form without skMLCKp, which presents multiple conformations. Most noticeably, the results indicate that binding of the target stabilizes the conformation of Ca^{2+}-bound CCMΔ5 resembling that of Ca^{2+}-bound CCM0 in the complex. Interestingly, the chemical shift position of M124 was shifted, and approached that of M144 of CCM0 in the complex. The peak of M109 was shifted to higher field in both ^{1}H and ^{13}C dimensions.

^{113}Cd-NMR

Based on the results of flow dialysis, LC-MS, and NMR titration experiments, the binding of the fourth Ca^{2+} ion to CCMΔ4 and CCMΔ5 should be weak. As the final NMR experiments, we tried one-dimensional ^{113}Cd-NMR to monitor the metal binding directly. ^{113}Cd is one of the NMR active nuclei, and it had been used as a probe in CaM studies[25–31]. Because the EF-hand motif can bind Cd^{2+} in the same manner as it binds Ca^{2+}, CaM binds four Cd^{2+} ions. It has been reported that target-free ^{113}Cd-saturated CaM gives rise to two peaks resonating from two EF3- and EF4-bound $^{113}Cd^{2+}$ ions. The other two ^{113}Cd ions that were bound to the N-lobe do not give observable peaks because of the exchange line broadening between bound- and free-states. Additionally, it has been reported that Cd^{2+}-saturated CaM can bind CaM targets and that four clear peaks are observed for the complex with skMLCKp.

The results of the ^{113}Cd-NMR experiments with CCM0, CCMΔ4, and CCMΔ5 are shown in Figure 10; data obtained in the absence of skMLCKp are shown on the left side. In

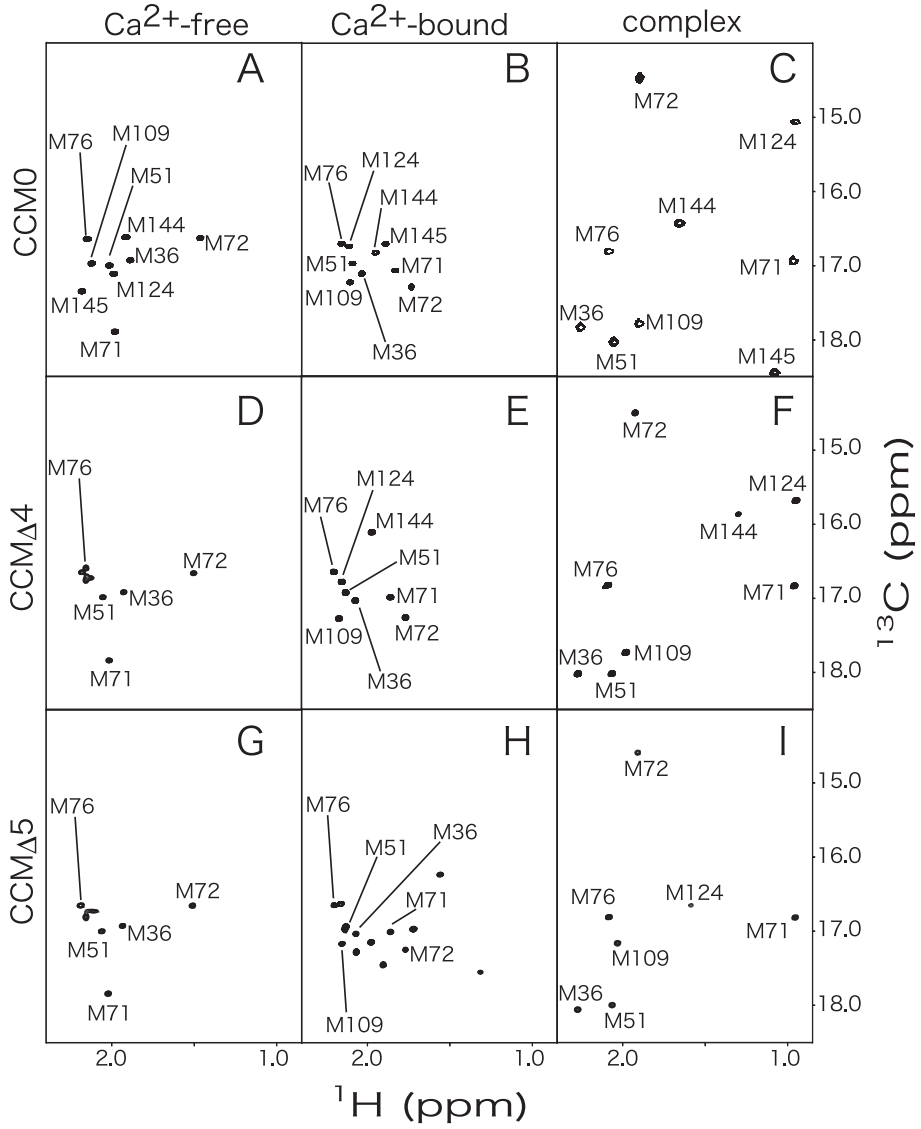

Figure 9 ^{1}H-^{13}C HSQC of selectively labeled-[^{13}C]-*methyl*-Met CaM and its variants. The panels (A)–(C), (D)–(F), and (G)–(I) represent the spectra for CCM0, CCMΔ4, and CCMΔ5, respectively. Panels (A), (D), and (G) represent the protein spectra in the absence of Ca^{2+}. (B), (E), and (H) are the protein spectra in the presence of Ca^{2+}. (C), (F), and (I) are the spectra of proteins complexed with the MLCK peptide. The assignments shown in panels (D)–(I) are similar to those in panels (A)–(C). All NMR data were recorded at ^{1}H frequency of 800 MHz.

the absence of the peptide, CCMΔ4 gave two peaks in the ^{113}Cd-NMR spectrum, indicating that the C-lobe of CCMΔ4 can still bind two ^{113}Cd ions; thus, CCMΔ4 binds four Ca^{2+} ions. This is consistent with the LC-MS results. However, the peak that appeared at higher field had some minor weak peaks at the bottom, suggesting the existence of conformational multiplicity in this EF-hand site. Unlike CCMΔ4, Cd^{2+}-saturated CCMΔ5 gave only one peak in the ^{113}Cd-NMR spectrum in the absence of the peptide (Figure 10E).

The data shown on the right-hand side of Figure 10 are ^{113}Cd-NMR spectra of the complexes. As previously reported, CCM0 gave four clear peaks in the presence of skMLCKp. Like CCM0, CCMΔ4 gave four peaks in the ^{113}Cd-NMR spectrum. The chemical shift positions of these four peaks were almost identical to those observed for CCM0 in the complex. Only one peak at the lowest field was slightly shifted to downfield, compared to the spectrum of CCM0. This result certainly indicates that Cd^{2+}-saturated CCMΔ4 can bind the peptide, forming a complex with a stable single conformation. Furthermore, the similarity of the spectra of CCM0 and CCMΔ4 in the peptide bound forms probably indicates the similarity of their conformations. On the other hand, Cd^{2+}-saturated CCMΔ5 in the presence of skMLCKp exhibited a unique spectrum in which two intense and two small peaks were observed. The chemical shifts were similar to those for CCM0, with the exception of the strong peak at the lowest field. This spectrum indicates that CCMΔ5 allows the binding of four Ca^{2+} ions, and that it

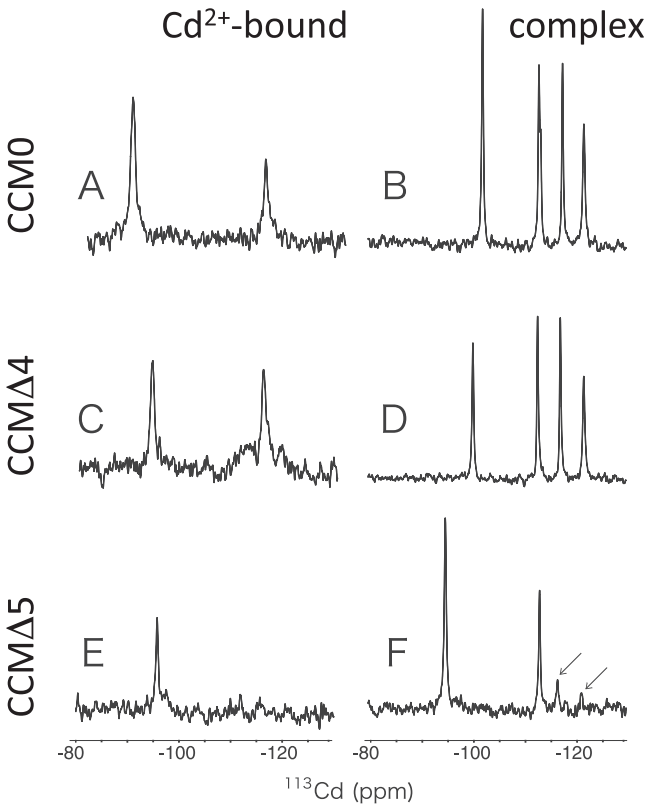

Figure 10 ^{113}Cd NMR of CaM and its variants. Panels (A) and (B), (C) and (D), and (E) and (F) represent the spectra for CCM0, CCMΔ4, and CCMΔ5, respectively. (A), (C), and (E) represent the protein spectra in the presence of Cd^{2+}. (B), (D), and (F) represent the protein spectra in the presence of Cd^{2+} and skMLCKp. All NMR data were recorded at ^{113}Cd resonance frequency of 110 MHz.

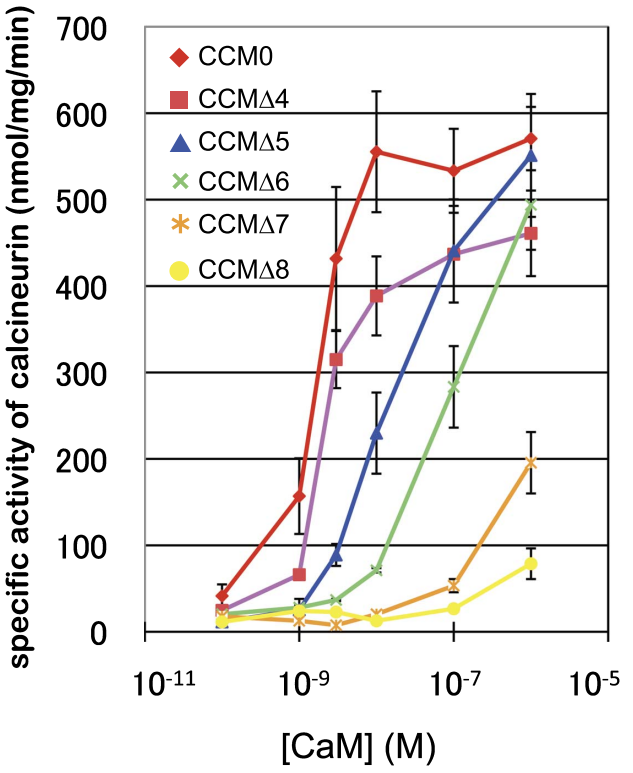

Figure 11 Target activation by CaM and its variants. Results of the CN pNPPase assay (n=3 and 2 for CCM0 and variants, respectively). CCM0, CCMΔ4, CCMΔ5, CCMΔ6, CCMΔ7, and CCMΔ8. Detailed experimental procedures are described in Materials and Methods.

binds skMLCKp through the two lobes. However, two of the four peaks were weak and slightly broad, which strongly suggests that the binding manner of Cd^{2+} to two of the EF-hand sites of CCMΔ5 in the complex is totally different from that of CCM0 and CCMΔ4. It was found that the spectrum was unchanged on addition of excess skMLCKp. Furthermore, the spectral change was undetectable at different sample temperatures ranging from 10 to 37°C. Thus, the conformation is relatively stable. This interpretation is supported by the results of ^{1}H-^{13}C HSQC of CCMΔ5 in the complex.

The ^{113}Cd-NMR data presented here provide tentative resonance assignments. In the absence of skMLCKp, a peak resonating at higher field is mainly affected by the C-terminal truncation of CaM. Thus, this resonance would be assigned to the Cd^{2+} ion bound to EF4. The peak at the lower field would be assigned to the Cd^{2+} ion bound to EF3. Assignment of the four peaks in the spectra to the samples in the complex with skMLCKp is exceedingly difficult. In the CCMΔ5 spectrum, two small peaks were detected. With moderate interpretation, these could be assigned to the two Cd^{2+} ions bound to the C-lobe. However, these assignments are inconsistent with the results reported in some previous studies[24,25,30]. In the previous studies, the experiments had been performed using a truncated fragment spanning EF1 and EF3. The isolated EF3 of the mutant, which may cause unexpected dimerization at high concentrations in the solution[32,33], was probably one of the reasons for the previous unreliable assignments.

Target activation

Finally, we measured the biological activity of intact CaM and its variants (Figure 11). In the biochemical experiments, we employed CN as a CaM target. CCMΔ4 and CCMΔ5 seemed to activate CN to the same extent as intact CaM. The apparent affinity for CN decreased with an increase in the deletion at the C-terminal. Interestingly, CCMΔ4 showed slightly lower activation compared with intact CaM, suggesting that M144 may have a specific role in CN activation. Even CCMΔ6 retained ability to activate CN. This is also an interesting finding, because it lacks the two Met residues, M144 and M145, contributing to the target binding[7,8]. In contrast, CCMΔ7 slightly activated CN, and CCMΔ8 lost the ability of target activation.

Discussion

In this study, we prepared a series of C-terminal deletion

mutants of CaM and investigated their structural and functional characteristics. We found that truncation of C-terminal residues largely changed the properties of CaM, suggesting that the C-terminal residues of CaM play important roles in its structure and function.

Ca^{2+} binding

The mutant CCMΔ4 lacks $M^{145}TAK^{148}$, which corresponds to approximately one turn of the α-helix, but retains seven residues ($Y^{138}EEFVQM^{144}$) of the F-helix of EF4. The LC-MS results show that, even in the absence of the CaM target, CCMΔ4 could bind four Ca^{2+} ions. Thus, truncation of the last four residues, $M^{145}TAK^{148}$, does not suppress, but reduces the Ca^{2+}-binding ability at EF4. The ^{113}Cd-NMR indicates that the EF4 of CCMΔ4 without the peptide can bind Ca^{2+} but has minor conformers. This is the reason why the EF4 of CCMΔ4 has weaker Ca^{2+}-affinity compared to that of intact CaM. As suggested from the flow-dialysis experiment, the affinity for Ca^{2+} at EF3 is also affected, the reason being that EF3 is coupled with EF4. As shown in the results of CCMΔ4, EF1, 2, and 3 have similar Ca^{2+}-affinity and EF4 becomes a weaker Ca^{2+}-binding site. ^{1}H-NMR titration of CCMΔ4 suggested the existence of intermediate structure(s) in both lobes during Ca^{2+}-induced structural transition. Thus, the last four residues, $M^{145}TAK^{148}$, have some role in inter-domain communication during Ca^{2+}-induced structural transition.

^{113}Cd-NMR indicates that deletion at M144 dramatically decreased the Ca^{2+} affinity of the C-lobe. The LC-MS results also suggest that CCMΔ5 binds four Ca^{2+} ions but a few are $3Ca^{2+}$-CCMΔ5 and $2Ca^{2+}$-CCMΔ5. ^{1}H-NMR titration experiments cannot provide further interpretation of the Ca^{2+}-binding order of the four EF hand sites in CCMΔ5, because the Ca^{2+}-bound form shows conformational multiplicity. However, all the results obtained here indicate that M144 plays a key role in attaining Ca^{2+}-induced conformational change at EF4 and contributes to stabilization of the Ca^{2+}-bound structure.

Structural stability

In the absence of Ca^{2+}, interaction between T146 and E82 is essential for stabilization of the C-lobe[9,34]. The present ^{1}H-^{15}N HSQC results of apo-CCMΔ4 and apo-CCMΔ5, where both are lacking T146, suggested that their C-lobes become unstable, although the N-lobes are in the proper conformation. The stability of their N-lobes may be retained by the interaction between the N-lobes and the central helix as reported previously[34–36]. It has been reported that oxidation of M144 and M145 disturbs the structure of CaM, suggesting that these residues are responsible for structural stability[37,38]. The results of present study provided further evidence that the effect of the two Met residues on the structural stability is limited to the C-lobe in the absence of Ca^{2+}.

In the presence of Ca^{2+}, CCMΔ4 is in a stable conformation, except for the truncated F-helix of EF4. Unlike CCMΔ4, a large part of CCMΔ5 is destabilized. The results suggest that the F-helix requires a minimum of seven residues ($Y^{138}EEFVQM^{144}$) to form a suitable Ca^{2+}-bound EF-hand structure in the absence of its targets.

The results of our CD experiments suggest that truncation of five or more residues suppresses large Ca^{2+}-induced conformational changes, implying that CCMΔ5, CCMΔ6, CCMΔ7, and CCMΔ8 have less sensitivity for Ca^{2+} binding. We assume that this insensitivity is due to the structural instability caused by the truncation. In fact, the ^{1}H-^{15}N HSQC spectrum of CCMΔ8, the shortest variant used in this study, shows a largely unstructured conformation (data not shown).

The peaks of I27, I100, and N137, which appeared down field in ^{1}H dimension in ^{1}H-^{15}N HSQC upon Ca^{2+} binding, are good indicators of the formation of antiparallel β-sheets connecting the two EF-hand loops in the two lobes. In the case of CCMΔ4, these signals were observed at their original positions, indicating that the four-residue truncation at the C-terminus does not affect the entire structure of CaM. However, Ca^{2+}-bound CCMΔ5 gives multiple peaks for I100 and N137 and a weak peak for I27. This also indicates that the five-residue ($M^{144}MTAK^{148}$) truncation at the C-terminus destabilizes not only the C-lobe, but also the N-lobe. Although the two lobes of the intact CaM are structurally independent, the five-residue truncation appears to affect the entire Ca^{2+}-bound molecule.

The findings prompted us to propose a hypothesis that M144 is a key factor in inter-domain communication in the Ca^{2+}-bound state. Such inter-domain coupling and/or communication are reported in previous papers[34–36,39]. A lack of M144 destabilizes the structure of the C-lobe, which might disturb the inter-domain couplings and result in destabilization of both the N- and C-lobes. This scenario may be supported by the results of ^{13}C-edited NOESY of Ca^{2+}-bound selectively labeled-[^{13}C]-*methyl*-Met samples in the absence of targets in which many NOE cross peaks are observed for CCMΔ4, but not for CCMΔ5 (data not shown). Further NMR study is now in progress.

Conformation of the complexes

In the current study, CN and skMLCKp were used as CaM targets. Both targets bind CaM through the 1-8-14 motif[7,40]. These numbers correspond to positions of the hydrophobic residues that are located in the CaM-binding region of the enzymes and are responsible for the binding to CaM. In the classical 1-8-14 binding model, both M144 and M145 in Ca^{2+}-bound CaM interact with a hydrophobic residue situated in the target peptide at position 1. Mutagenesis experiments have shown that replacement of one of these Met residues by Leu does not affect target activation for CN[41]. Accordingly, it is believed that the presence of at least one of these Met residues, that is, M144 or M145, is sufficient for activation of the target through the 1-8-14 motif. In fact, the NMR studies revealed that CCMΔ4, which lacks

M145, forms a complex with the target. The two lobes of CCMΔ4 interact with the skMLCK peptide in a complex structure that is expected to be similar to that of CCM0. This suggests that the four C-terminal residues, including M145, do not play a significant role in the formation of complexes with a 1-8-14 binding motif. We unexpectedly found that CCMΔ5, which lacks both M144 and M145, binds four Ca^{2+} ions and activates CN. It is thought that binding of the target to the C-lobe immobilizes the truncated last helix, and therefore, EF4 gains some affinity for Ca^{2+}. However, the ^{113}Cd-NMR results suggest that the metal binding mode of two of the four EF-hand sites of skMLCKp-bound CCMΔ5 is completely different from that of CCM0 because the ^{113}Cd-NMR spectrum showed two sharp strong peaks and two weak peaks. Since the C-terminal residues are truncated, the weak peaks are likely to be $^{113}Cd^{2+}$ ions bound to the C-lobe. The strong peak at the lowest chemical shift was moved to lower field compared to that of CCM0. When we assign the two strong peaks to the $^{113}Cd^{2+}$ ions bound to the N-lobe, the structure of the N-lobe in the complex is expected to be slightly different from that of CCM0. In addition, it is interesting to note that the chemical shift of M124 methyl resonance in ^{1}H-^{13}C HSQC for CCMΔ5 in the complex was very close to that of M144 for CCM0. This suggests that the M124 of CCMΔ5 may replace the role of M144 in interacting with the target residue at position 1. Further NMR characterization of Ca^{2+}-saturated CCMΔ5 in the presence of skMLCKp is now in progress.

Target activation

We investigated the capacity of the different CaM variants to activate CN and found that CCMΔ4 exhibits a decreased capacity for target activation. Further deletion of the C-terminal residues decreased the apparent affinity for CN to recover the estimated maximum activity of native CaM, and CCMΔ8 almost completely lost its ability to activate the target because of its incomplete Ca^{2+}-bound conformation. Unpredictably, CCMΔ6 displayed relatively higher ability for CN activation, probably meaning that the C-lobe of Ca^{2+}-saturated CCMΔ6, lacking both M144 and M145, still has some ability to interact with CN. The present results might seem inconsistent with the previous mutagenesis experiments, suggesting that at least one of these two Met residues is necessary for gaining the activity of CN[41]. CCMΔ7 showed lower ability to activate CN. Thus, the seventh residue, V142, from the C-terminus might play a key role for CN activation in CCMΔ6. At present, two possible roles could be proposed for V142 in CCMΔ6. One is that V142 contributes to stabilize the overall conformation of the C-lobe via the interaction with other residues of CCMΔ6. The other is that the hydrophobic side chain of V142 directly binds the target after reorientation of the short F-helix of EF4, although V142 is not involved into target interaction in the CaM-skMLCK peptide complex[7].

As discussed in the previous section, M144 would play a key role in stabilizing the C-terminal helix and the overall conformation of CaM. Moreover, the stable C-terminal α-helix may contribute to determining the apparent affinity for CN. Apparently, M144 in CCMΔ4 has a role in decreasing the activity of CN. This obvious inhibitory effect of M144 may be caused by the structural rearrangements required to achieve a stable conformation (Figure 8). Previous Met to Leu single-mutation experiments have shown that M144L and M145L do not play a significant role in the activation of smMLCK, CN, or phosphodiesterase. However, the double mutant [M144R, M145L]-CaM exhibits very low phosphodiesterase activity[41,42]. Our present results show that M144 plays a key role in stabilizing the C-terminal α-helix and the overall conformation of Ca^{2+}-bound CaM that is essential for its function.

Acknowledgments

The authors thank Professor Michio Yazawa of Hokkaido University for his helpful suggestions and fruitful discussions. The authors also thank the technicians at the Center for Nano Materials and Technology (CNMT), Japan Advanced Institute of Science and Technology (JAIST) for their help with the maintenance of the NMR magnets used in this study. The authors express thanks to Kyoto-Sentan Nanotech Network operated by Japan Science and Technology Agency (JST) for the financial support to maintain the NMR machines.

References

1. Hoeflich, K. P. & Ikura, M. Calmodulin in action: diversity in target recognition and activation mechanism. *Cell* **108**, 739–742 (2002).
2. Chin, D. & Means, A. R. Calmodulin: a prototypical calcium sensor. *Trends Cell Biol.* **10**, 322–328 (2000).
3. Yap, K. L., Kim, J., Truong, K., Sherman, M., Yuan, T. & Ikura, M. Calmodulin target database. *J. Struct. Funct. Genomics* **1**, 8–14 (2000).
4. Babu, Y. S., Bugg, C. E. & Cook, W. J. Structure of calmodulin refined at 2.2 Å resolution. *J. Mol. Biol.* **204**, 191–204 (1988).
5. Chang, S. L., Szabo, A. & Tjandra, N. Temperature dependence of domain motions of calmodulin probed by NMR relaxation at multiple fields. *J. Am. Chem. Soc.* **125**, 11379–11384 (2003).
6. Ikura, M., Hiraoki, T., Hikichi, K., Minowa, O., Yamaguchi, H., Yazawa, M. & Yagi, K. Nuclear magnetic resonance studies on calmodulin. *Biochemistry* **23**, 3124–3128 (1984).
7. Ikura, M., Clore, G. M., Gronenborn, A. M., Zhu, G., Klee, C. B. & Bax, A. Solution structure of a calmodulin-target peptide complex by multidimensional NMR. *Science* **256**, 632–638 (1992).
8. Meador, W. E., Means, A. R. & Quiocho, F. A. Modulation of calmodulin plasticity in molecular recognition on the basis of X-ray structures. *Science* **262**, 1718–1721 (1993).
9. Kuboniwa, H., Tjandra, N., Grzesiek, S., Ren, H., Klee, C. B. & Bax, A. Solution structure of calcium-free calmodulin. *Nat. Struct. Biol.* **2**, 768–776 (1995).
10. Zhang, M., Tanaka, T. & Ikura, M. Calcium-induced confor-

mational transition revealed by the solution structure of apo calmodulin. *Nat. Struct. Biol.* **2**, 758–767 (1995).
11. James, P., Vorherr, T. & Carafoli, E. Calmodulin-binding domains: just two faced or multi-faceted? *Trends Biochem. Sci.* **20**, 38–42 (1995).
12. Davis, T. N., Urdea, M. S., Masiarz, F. R. & Thorner, J. Isolation of the yeast calmodulin gene: calmodulin is an essential protein. *Cell* **47**, 423–431 (1986).
13. Luan, Y., Matsuura, I., Yazawa, M., Nakamura, T. & Yagi, K. Yeast calmodulin: structural and functional differences compared with vertebrate calmodulin. *J. Biochem.* **102**, 1531–1537 (1987).
14. Matsuura, I., Ishihara, K., Nakai, Y., Yazawa, M., Toda, H. & Yagi, K. A site-directed mutagenesis study of yeast calmodulin. *J. Biochem.* **109**, 190–197 (1991).
15. Matsuura, I., Kimura, E., Tai, K. & Yazawa, M. Mutagenesis of the fourth calcium-binding domain of yeast calmodulin. *J. Biol. Chem.* **268**, 13267–13273 (1993).
16. Nakashima, K. Ph.D. thesis (Hokkaido Univ.) (1999).
17. Nakashima, K., Ishida, H., Ohki, S., Hikichi, K. & Yazawa, M. Calcium binding induces interaction between the N- and C-terminal domains of yeast calmodulin and modulates its overall conformation. *Biochemistry* **38**, 98–104 (1999).
18. Ohki, S., Ikura, M. & Zhang, M. Identification of Mg^{2+} binding sites and the role of Mg^{2+} on target recognition by calmodulin. *Biochemistry* **36**, 4309–4316 (1997).
19. Yazawa, M., Vorherr, T., James, P., Carafoli, E. & Yagi, K. Binding of calcium by calmodulin: influence of the calmodulin binding domain of the plasma membrane calcium pump. *Biochemistry* **31**, 3171–3176 (1992).
20. Yazawa, M. Quantitative analysis of Ca^{2+}-binding by flow dialysis. *Methods Mol. Biol.* **173**, 3–14 (2002).
21. Delaglio, F., Grzesiek, S., Vuister, G. W., Zhu, G., Pfeifer J. & Bax A. NMRPipe: a multidimensional spectral processing system based on UNIX pipes. *J. Biomol. NMR.* **3**, 277–293 (1995).
22. Haiech, J., Klee, C. B. & Demaille, J. G. Effects of cations on affinity of calmodulin: ordered binding of calcium ions allows the specific activation of calmodulin-stimulated enzymes. *Biochemistry* **20**, 3890–3897 (1981).
23. Zhang, M. & Vogel, H. J. The calmodulin-binding domain of caldesmon binds to calmodulin in an alpha-helical conformation. *Biochemistry* **33**, 1163–1171 (1994).
24. Siivari, K., Zhang, M., Palmer III, A. G. & Vogel, H. J. NMR studies of the methionine methyl group in calmodulin. *FEBS Lett.* **366**, 104–108 (1995).
25. Forsén, S., Thulin, E., Drakenberg, T., Krebs, J. & Seamon, K. A ^{113}Cd-NMR study of calmodulin and its interaction with calcium, magnesium and trifluoperazine. *FEBS Lett.* **117**, 189–194 (1980).
26. Andersson, A., Forsén, S., Thulin, E. & Vogel, H. J. Cadmium-113 nuclear magnetic resonance studies of proteolytic fragments of calmodulin: assignment of strong and weak cation binding sites. *Biochemistry* **22**, 2309–2313 (1983).
27. Thulin, E., Anderson, A., Drakenberg, T., Forsén, S. & Vogel, H. J. Metal ion and drug binding to proteolytic fragments of calmodulin: proteolytic, cadmium-113, and proton nuclear magnetic resonance studies. *Biochemistry* **23**, 1862–1870 (1984).
28. Linse, S., Drakenberg, T. & Forsén, S. Mastoparan binding induces a structural change affecting both the N-terminal and C-terminal domain of calmodulin. A ^{113}Cd-NMR study. *FEBS Lett.* **199**, 28–32 (1986).
29. Ikura, M., Hasegawa, N., Aimoto, S., Yazawa, M. & Hikichi, K. ^{113}Cd-NMR evidence for cooperative interaction between amino- and carboxyl-terminal domains of calmodulin. *Biochem. Biophys. Res. Commun.* **161**, 1233–1238 (1989).
30. Ohki, S., Iwamoto, U., Aimoto, S., Yazawa, M. & Hikichi, K. Mg^{2+} inhibits formation of $4Ca^{2+}$-calmodulin-enzyme complex at lower Ca^{2+} concentration. ^{1}H and ^{113}Cd NMR studies. *J. Biol. Chem.* **268**, 12388–12392 (1993).
31. Zhang, M., Yuan, T., Aramini, J. M. & Vogel, H. J. Interaction of calmodulin with its binding domain of rat cerebellar nitric oxide synthase. A multinuclear NMR study. *J. Biol. Chem.* **270**, 20901–20907 (1995).
32. Reid, R. E. A synthetic 33-residue analogue of bovine brain calmodulin calcium binding site III: synthesis, purification, and calcium binding. *Biochemistry* **26**, 6070–6073 (1987).
33. Kay, L. E., Forman-Kay, J. D., McCubbin, W. D. & Kay, C. M. Solution structure of a polypeptide dimer comprising the fourth Ca^{2+}-binding site of troponin C by nuclear magnetic resonance spectroscopy. *Biochemistry* **30**, 4323–4333 (1991).
34. Faga, L. A., Sorensen, B. R., VanScyoc, W. S. & Shea, M. A. Basic interdomain boundary residues in calmodulin decrease calcium affinity of sites I and II by stabilizing helix-helix interactions. *Proteins: Structure, Function, and Genetics* **50**, 381–391 (2003).
35. Sorensen, B. R., Faga, L. A., Hultman, R. & Shea, M. A. An interdomain linker increases the thermostability and decreases the calcium affinity of the calmodulin N-domain. *Biochemistry* **41**, 15–20 (2002).
36. Chen, B., Lowry, D. F., Mayer, M. U. & Squier, T. C. Helix A stabilization precedes amino-terminal lobe activation upon calcium binding to calmodulin. *Biochemistry* **47**, 9220–9226 (2008).
37. Gao, J., Yin, D. H., Yao, Y., Sun, H., Qin, Z., Schöneich, C., Williams, T. D. & Squier, T. C. Loss of conformational stability in calmodulin upon methionine oxidation. *Biophys. J.* **74**, 1115–1134 (1998).
38. Ferrington, D. A., Sun, H., Murray, K. K., Costa, J., Williams, T. D., Bigelow, D. J. & Squier, T. C. Selective degradation of oxidized calmodulin by the 20 S proteasome. *J. Biol. Chem.* **276**, 937–943 (2001).
39. Bartlett, R. K., Urbauer, J. B., Anbandam, A., Smallwood, H. S., Urbauer, J. L. & Squier, T. C. Oxidation of Met144 and Met145 in calmodulin blocks calmodulin dependent activation of the plasma membrane Ca-ATPase. *Biochemistry* **42**, 3231–3238 (2003).
40. Ye, Q., Wang, H., Zheng, J., Wei, Q. & Jia, Z. The complex structure of calmodulin bound to a calcineurin peptide. *Proteins* **73**, 19–27 (2008).
41. Edwards, R. A., Walsh, M. P., Sutherland, C. & Vogel, H. J. Activation of calcineurin and smooth muscle myosin light chain kinase by Met-to-Leu mutants of calmodulin. *Biochem. J.* **331**, 149–152 (1998).
42. Zhang, M., Li, M., Wang, J. H. & Vogel, H. J. The effect of Met $\rightarrow$ Leu mutation on calmodulin's ability to activate cyclic nucleotide phosphodiesterase. *J. Biol. Chem*. **269**, 15546–15552 (1994).